Observation of Motion-Dependent Nonlinear Dispersion with Narrow-Linewidth Atoms in an Optical Cavity

Philip G. Westergaard,[1,2,*] Bjarke T. R. Christensen,[1] David Tieri,[3] Rastin Matin,[1] John Cooper,[3] Murray Holland,[3] Jun Ye,[3] and Jan W. Thomsen[1]

[1]*Niels Bohr Institute, University of Copenhagen, Blegdamsvej 17, 2100 Copenhagen, Denmark*
[2]*Danish Fundamental Metrology, Matematiktorvet 307, 1 sal, 2800 Kongens Lyngby, Denmark*
[3]*JILA, National Institute of Standards and Technology and University of Colorado, Boulder, Colorado 80309-0440, USA*

(Received 15 August 2014; revised manuscript received 26 January 2015; published 4 March 2015)

As an alternative to state-of-the-art laser frequency stabilization using ultrastable cavities, it has been proposed to exploit the nonlinear effects from coupling of atoms with a narrow transition to an optical cavity. Here, we have constructed such a system and observed nonlinear phase shifts of a narrow optical line by a strong coupling of a sample of strontium-88 atoms to an optical cavity. The sample temperature of a few mK provides a domain where the Doppler energy scale is several orders of magnitude larger than the narrow linewidth of the optical transition. This makes the system sensitive to velocity dependent multiphoton scattering events (Dopplerons) that affect the cavity field transmission and phase. By varying the number of atoms and the intracavity power, we systematically study this nonlinear phase signature which displays roughly the same features as for much lower temperature samples. This demonstration in a relatively simple system opens new possibilities for alternative routes to laser stabilization at the sub–100 mHz level and superradiant laser sources involving narrow-line atoms. The understanding of relevant motional effects obtained here has direct implications for other atomic clocks when used in relation to ultranarrow clock transitions.

DOI: 10.1103/PhysRevLett.114.093002 PACS numbers: 32.80.Wr, 37.30.+i, 42.50.Ct, 42.62.Fi

State-of-the-art atomic clocks rely on highly coherent light sources to probe narrow optical transitions [1–5]. However, these clocks are limited by the frequency noise of the interrogation oscillator through the Dick effect [6]. Only recently, multiatom optical clocks have surpassed single ion clocks in stability owing to enhanced laser stability [1,2,7]. Achieving a better stability has, so far, been hampered by thermal noise in the reference cavity used for laser stabilization [8–10]. Recent proposals suggest an alternative approach to laser stabilization [11–13] where atoms in an optical lattice are probed on the narrow clock transition inside an optical cavity. This brings nonlinear effects into the system dynamics that could considerably enhance the spectral sensitivity and could potentially lead to laser stability comparable to or better than the current state of the art. However, for finite temperature samples of atoms, the principal mechanisms that are relevant to this physical domain have not been investigated in detail.

In such systems with highly nonlinear phase response, *a priori* unpredictable effects such as bistability [13] and the finite temperature of the atomic ensemble can change the phase response in an undesirable way, which could reduce the performance of the stabilization scheme for all practical implementations. To achieve a better understanding of cavity-mediated effects with a narrow optical transition, we have constructed a system with ^{88}Sr atoms probed on the $|^1S_0\rangle - |^3P_1\rangle$ transition at 689 nm inside an optical cavity (see Fig. 1). To capture the basic physics of the strong nonlinear phenomena, one can consider N atomic dipoles strongly coupled to a single mode of the cavity field. The dipole moment associated with this narrow transition is around 5 orders of magnitude smaller than that for a typical dipole-allowed transition in an alkaline element. Also, at finite temperature only a small fraction of the atomic sample is probed due to Doppler broadening. Here, the role of the cavity is to enhance the weak interaction by order of the finesse of the cavity.

Experimentally we operate in the so-called bad cavity regime, where the atomic dipole decay rate is a factor of 1000 smaller than the cavity decay rate κ. In our experiment we use the $^{88}\mathrm{Sr}|5s^{21}S_0\rangle - |5s5p^1P_1\rangle$ transition at 461 nm to cool and trap atoms in a magneto-optical trap (MOT). We load about 5×10^8 atoms in the MOT at a temperature of 2–4 mK inside an optical cavity prepared for light at 689 nm. The cavity waist of $w_0 = 500$ μm ensures a good overlap with the MOT and negligible transit time broadening (~2 kHz) compared to the natural linewidth ($\Gamma/2\pi =$ 7.6 kHz) of the probe transition. The dimensionless number $C = C_0N$, where $C_0 = 4g^2/\Gamma\kappa$ depends on the single atom–cavity coupling constant g, is known as the collective cooperativity and is a measure of how strong the coherent atom-cavity coupling is with respect to the dissipation channels. In our configuration ($g/2\pi = 590$ Hz, $\kappa/2\pi =$ 5.8 MHz) we are able to generate a collective cooperativity of about $C = 630$, thus placing our system in the regime of high collective cooperativity in the bad cavity limit, but

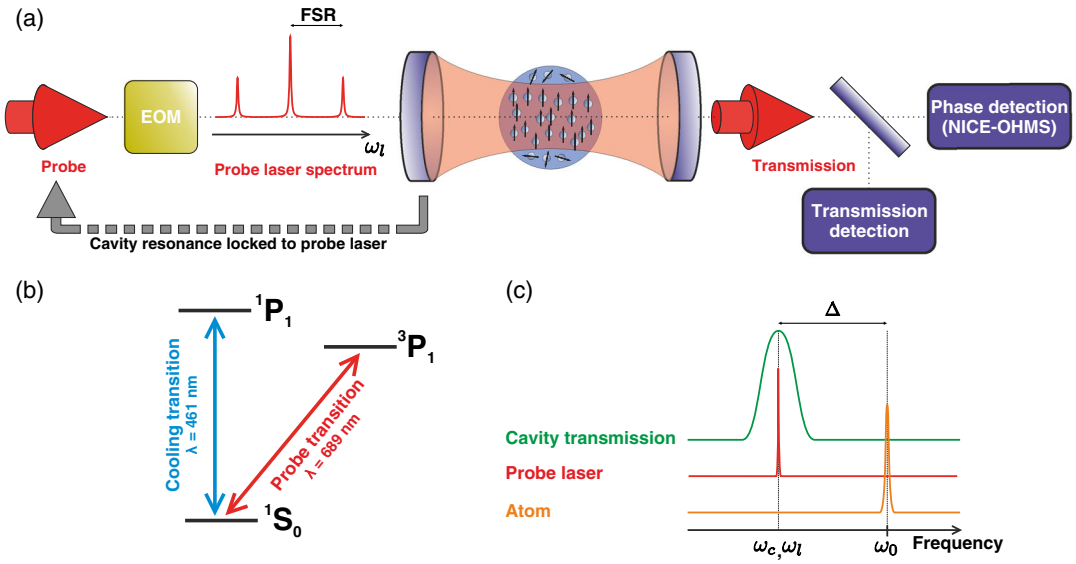

FIG. 1 (color online). (a) Experimental setup. A sample of cold atoms (MOT) is prepared inside a low finesse cavity ($F = 85$) which is held at resonance with the probe laser. We probe the atoms on the intercombination line $|5s^2\,{}^1S_0\rangle - |5s5p\,{}^3P_1\rangle$ at 689 nm ($\Gamma/2\pi = 7.6$ kHz). Both intensity and phase shift of the transmitted probe light are recorded. The phase is measured relative to the input field by employing cavity-enhanced heterodyne spectroscopy (NICE-OHMS). (b) Energy levels of the ^{88}Sr atom and transitions relevant to this work. (c) Relation between the spectral components in the experiment. The probe laser frequency ω_l (and consequently the cavity resonance ω_c) is detuned a variable amount Δ with respect to the atomic resonance ω_0.

outside the more restrictive cavity QED strongly coupled regime [14,15].

Our experiment is operated in a cyclic fashion. We start each cycle preparing the atomic sample by loading a MOT inside the optical cavity. After loading we shut off the MOT beams and probe the atoms at 689 nm while recording both the intensity and the phase shift of the transmitted probe light via two detectors (see Fig. 1). The total cycle time is typically around 0.5–1 s. For the phase measurement we employ cavity-enhanced FM spectroscopy by using the so-called noise-immune cavity-enhanced optical-heterodyne molecular spectroscopy (NICE-OHMS) technique [19,20] (see the Supplemental Material [15]). This technique has a clear advantage over heterodyne signals generated, for example, from interferometric methods in terms of superior noise reduction and simplicity. During experiments we lock the cavity resonance to the 689 nm laser frequency using a Hänsch-Couillaud scheme [21]. The standing wave generated in the cavity will thus be present at all times while the 689 nm laser frequency is scanned.

In the limit of $T = 0$ and for very low cavity field intensities several solutions exist for the steady-state intracavity field [13]. This is known as optical bistability, which would render the system unsuited for frequency stabilization. However, at finite temperatures when motional effects are included, this picture changes. In this case, there is a critical temperature T_{crit} above which only one solution for the steady-state intracavity field exists. For our parameters, T_{crit} is of the order of a few hundred nK, while experiments are typically performed at mK temperatures.

The nonzero velocity of the atoms brings additional photon resonance phenomena into play, which changes the complex amplitude of the cavity field around the atomic resonance ω_0. In the rest frame of an atom moving with velocity v_j the atom experiences a bichromatic light field given by $\omega_+ = \omega_l(1 + v_j/c)$ and $\omega_- = \omega_l(1 - v_j/c)$, where ω_l is the laser frequency and c is the speed of light. Resonant scattering events will take place if the atom is Doppler tuned into resonance at ω_0, e.g., $\omega_- = \omega_0$, such that the atom may absorb a photon from a given direction of the cavity field. Higher order resonances are also possible where, e.g., the atom absorbs two photons from one direction at ω_- and emits one photon in the other direction at ω_+. Generally, the resonance condition for $p + 1$ absorbed and p emitted photons becomes $(p + 1)\omega_- = \omega_0 + p\omega_+$ for $p = 0, 1, 2, \ldots$ [22]. The process is illustrated in Fig. 2(a). These nonlinear multiphoton scattering effects are known as Dopplerons and give rise to a series of velocity dependent resonances [23] which change the transmitted field amplitude around resonance.

In Figs. 2(b) and 2(c) we show typical results for a frequency scan across the $|^1S_0\rangle - |^3P_1\rangle$ line resonance (red circles). The input power was 975 nW, corresponding to an average saturation parameter of $S_0 = 618$. It is clear that the phase signal in Fig. 2(c) has a significantly higher signal-to-noise ratio (SNR = 70) than the transmitted power signal in Fig. 2(b) (SNR ~ 4), demonstrating the effectiveness of the NICE-OHMS technique. Currently, the factor limiting the signal-to-noise ratio of the phase signal is the shot-to-shot atom number fluctuations and

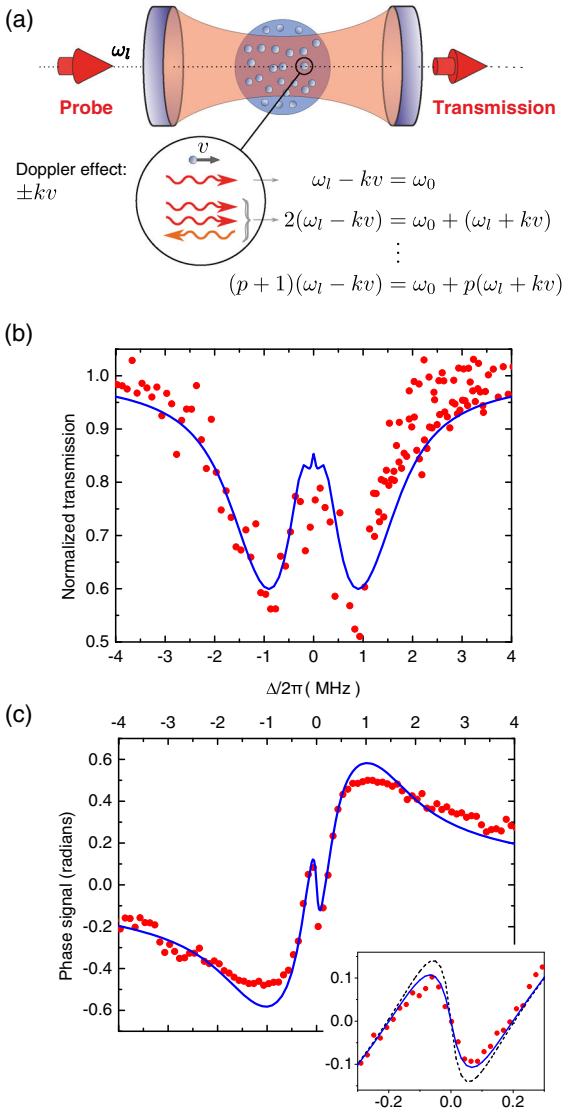

FIG. 2 (color online). (a) Illustration of the Doppleron multiphoton processes that take place in our system. We consider a given atom with velocity component v in the direction of the cavity axis. The first resonance condition (the top equation) involves only one photon and corresponds to the usual Doppler effect. The next resonance involves two photons absorbed and one photon emitted, and so forth. (b),(c) Typical frequency scan without any averaging across the atomic resonance for an input power of 975 nW and a total number of atoms in the MOT of $N = 4.4 \times 10^8$. The data in (b) display the transmission of the probe light through the cavity normalized to a signal with no atoms in the cavity. The data in (c) is the phase shift of the cavity-transmitted field obtained using the NICE-OHMS method. The solid lines are theoretical predictions based on our theoretical model, which includes the Doppler effect and the spatial overlap of the thermal cloud (here with temperature $T = 2.3$ mK) with the cavity field. At maximum phase shift (around detunings of $\Delta \simeq \pm 1$ MHz), our detection system starts to saturate, giving a slightly flatter appearance of the phase data. (Inset) Zoom on central phase feature with similar experimental parameters [data are identical to Fig. 4(a)]. Here, we have included a theoretical plot that does not take the Dopplerons into account (black, dashed curve). The effect of the Dopplerons is readily apparent. Units on axes are the same as in (c).

residual amplitude modulation from the electro-optic modulator (EOM).

We model the dynamics of the system by a Hamiltonian describing the coherent time evolution of an ensemble of atoms, where each atom with a given velocity is coupled to a single mode of the optical cavity. Solving the corresponding optical Bloch equations yields the cavity-transmitted intensity and phase as a function of detuning, number of atoms, and temperature. Our model is also adapted to take into account the spatial extent of the cavity field and the atomic density profile. The blue solid curves in Figs. 2(b) and 2(c) represent the theoretical prediction based on the Hamiltonian presented in Eq. 2 of the Supplemental Material [15]. In our theoretical model we fix the number of atoms, laser input power, laser linewidth, cavity waist, and cavity finesse based on experimental values, but allow a scaling factor for the absolute phase. The temperature is allowed to vary in the range of 2–4 mK, in accordance with the experimental condition.

Considering the transmission in Fig. 2(b), we can identify three spectral features: (1) the broad (∼3 MHz wide) Doppler absorption feature consistent with the sample temperature of a few mK; (2) a central region (∼1 MHz wide) with enhanced transmission due to saturation, affected by the Doppleron resonances which lead to enhanced backscattering (or reduced forward transmission), limiting the height of the saturated absorption peak; (3) finally, in the central region around zero velocity (i.e., on resonance), the Doppleron mechanism breaks down and the saturated absorption takes place again with increased transmission as a result.

The Dopplerons also have an effect in the phase signal [Fig. 2(c)], although the effect is negligible for large laser detunings corresponding to larger atom velocities. In the inset of Fig. 2(c), we zoom in on the phase of the central saturated absorption feature where we have plotted experimental data [with parameters corresponding to Fig. 4(a)] and theoretical curves without Dopplerons (black, dashed line) and with Dopplerons (blue line). Here, the effect of Dopplerons becomes clear and there is an observable effect on the phase signature which is a decrease in slope around resonance, showing consistency between our theoretical model and the experimental data. This decrease in slope is important in the determination of the frequency stability that is achievable using this system since the stability depends inversely on the square of the slope around resonance, and reducing the temperature further does not significantly improve this slope [15].

To evaluate and characterize our physical system experimentally and test it against the theoretical model, we have mapped out the central phase feature as a function of probe input power with a fixed atom number. In addition to a validation of the theoretical model, this will provide an understanding of the behavior and sensitivity of the phase signal to typical experimental variables relevant to, e.g.,

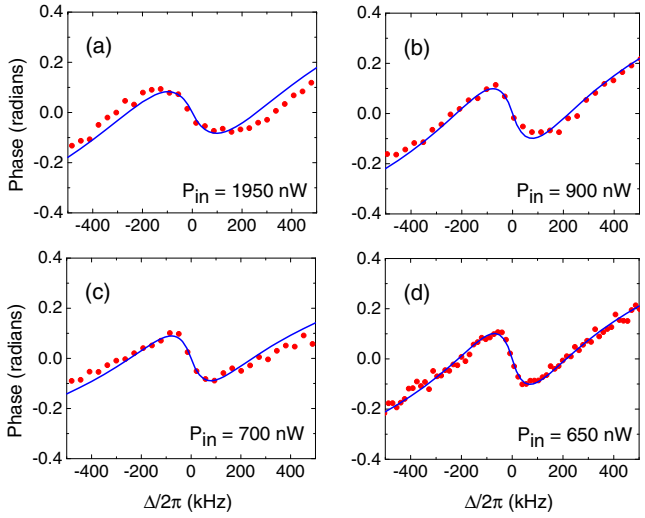

FIG. 3 (color online). Measured phase shift of the cavity-transmitted field when scanned across the atomic resonance. The input probe laser power P_{in} is progressively decreased from 1950 nW (a), 900 nW (b), 700 nW (c) to 650 nW (d). The number of atoms is about $N_{\text{cavity}} = 2.5 \times 10^7$. Each point is an average of three data points. The solid lines are theoretical predictions based on our theoretical model.

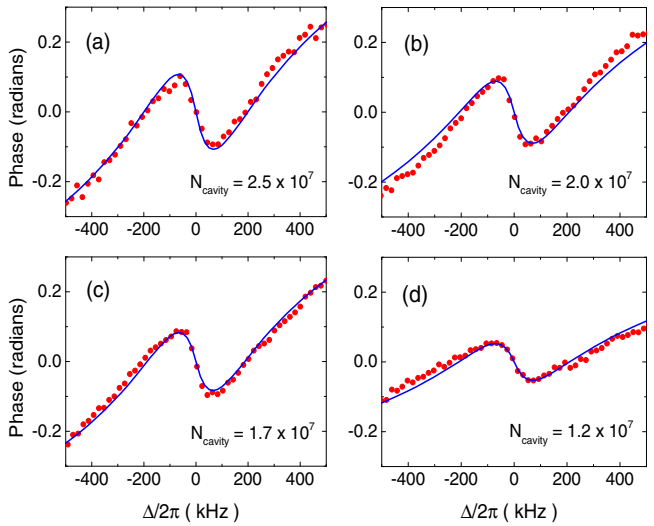

FIG. 4 (color online). Measured phase shift of the probe light when scanned across the atomic resonance. The number of atoms in the cavity is progressively decreased from 2.5×10^7 (a), 2.0×10^7 (b), 1.7×10^7 (c) to 1.2×10^7 (d). The input power used for all plots was 650 nW. Each point is an average of three data points. The solid lines are theoretical predictions based on our theoretical model. The central slope scales linearly with atom number.

laser stabilization. In Fig. 3 we show the phase signal for a fixed number of atoms as a function of laser detuning for different input powers in the range 650–1950 nW. For high input powers we strongly saturate the dipole and power broaden the central saturated absorption peak. As we gradually lower the input power, the power broadening is reduced, leaving the central phase feature with a larger slope without reducing the signal-to-noise ratio.

Figs. 4(a)–4(d) show the evolution of the phase signal for fixed probe power as the number of atoms inside the cavity mode is changed from $N_{\text{cavity}} = 2.5 \times 10^7$ in (a) to $N_{\text{cavity}} = 1.2 \times 10^7$ in (d). We observe a strong dependence on atom number with increasing phase response and increasing slope on resonance for increasing atom numbers, as expected, and the slope can straightforwardly be improved by increasing the number of atoms. However, our system is strongly nonlinear and other optimal parameters, such as input power, for a given number of atoms, may not be trivially assigned to our experiment, but must be found numerically or experimentally.

Using the central phase slope for laser frequency locking, we estimate a shot noise limited linewidth of 1000 mHz, based on our experimental parameters. This number can be improved by at least a factor of 20 with realistic improvements in the experimental parameters, e.g., by optimizing the EOM modulation index (a factor 15) and increasing the atom number and the cavity finesse (both a factor 10), which would render the system comparable to state-of-the-art frequency stabilization Refs. [9,24–26] (see the Supplemental Material [15] for details).

In conclusion, we have constructed a system dominated by highly saturated multiphoton absorption with laser-cooled strontium atoms coupled to a low finesse optical cavity. The transmission through the cavity is altered by thermal effects but, apart from a small decrease in slope, the central phase response of the atoms remains relatively immune to these effects while displaying a high SNR owing to the cavity and detection technique. The atomic phase signature was observed via cavity-enhanced FM spectroscopy (NICE-OHMS) on the narrow optical $|^1S_0\rangle - |^3P_1\rangle$ intercombination line of ^{88}Sr, providing a SNR exceeding 7000 for one second of integration. The understanding obtained here of the "bad cavity" physics lends promise to further development in this area, such as a new generation of frequency stabilization [11,13] or superradiant laser sources [27,28]. Specifically, the physical understanding of a "warm" system (MOT temperature) obtained in this work will prove valuable when future atomic clocks, stable lasers, or both will be operated under more noisy and compact environments—e.g., in vehicles and spacecrafts—where the size, ruggedness, and convenience of the setup might dictate higher atomic temperatures than what is currently used for state-of-the-art systems. In this situation, this work will serve as an important piece of technical understanding for out-of-lab clocks employing warm atoms.

We would like to acknowledge support from the Danish Research Council and ESA Contract No. 4000108303/13/NL/PA-NPI272-2012. D. T., M. H., and J. Y. also wish to thank the DARPA QuASAR program, NIST, and the NSF Physics Frontier Center at JILA for financial support.

*pgw@dfm.dk

[1] B. J. Bloom, T. L. Nicholson, J. R. Williams, S. L. Campbell, M. Bishof, X. Zhang, W. Zhang, S. L. Bromley, and J. Ye, Nature (London) **506**, 71 (2014).

[2] N. Hinkley, J. A. Sherman, N. B. Phillips, M. Schioppo, N. D. Lemke, K. Beloy, M. Pizzocaro, C. W. Oates, and A. D. Ludlow, Science **341**, 1215 (2013).

[3] R. Le Targat *et al.*, Nat. Commun. **4**, 2109 (2013).

[4] M. Takamoto, F.-L. Hong, R. Higashi, and H. Katori, Nature (London) **435**, 321 (2005).

[5] C. W. Chou, D. B. Hume, J. C. J. Koelemeij, D. J. Wineland, and T. Rosenband, Phys. Rev. Lett. **104**, 070802 (2010).

[6] G. Santarelli, C. Audoin, A. Makdissi, P. Laurent, G. J. Dick, and A. Clairon, IEEE Trans. Ultrason. Ferroelectr. Freq. Control **45**, 887 (1998).

[7] T. L. Nicholson, M. J. Martin, J. R. Williams, B. J. Bloom, M. Bishof, M. D. Swallows, S. L. Campbell, and J. Ye, Phys. Rev. Lett. **109**, 230801 (2012).

[8] T. Kessler, T. Legero, and U. Sterr, J. Opt. Soc. Am. B **29**, 178 (2012).

[9] T. Kessler, C. Hagemann, C. Grebing, T. Legero, U. Sterr, F. Riehle, M. J. Martin, L. Chen, and J. Ye, Nat. Photonics **6**, 687 (2012).

[10] M. J. Martin, M. Bishof, M. D. Swallows, X. Zhang, C. Benko, J. von-Stecher, A. V. Gorshkov, A. M. Rey, and J. Ye, Science **341**, 632 (2013).

[11] D. Meiser, J. Ye, D. R. Carlson, and M. J. Holland, Phys. Rev. Lett. **102**, 163601 (2009).

[12] D. Meiser and M. J. Holland, Phys. Rev. A **81**, 033847 (2010).

[13] M. J. Martin, D. Meiser, J. W. Thomsen, J. Ye, and M. J. Holland, Phys. Rev. A **84**, 063813 (2011).

[14] H. Tanji-Suzuki, I. D. Leroux, M. H. Schleier-Smith, M. Cetina, A. Grier, J. Simon, and V. Vuletic, Adv. At. Mol. Opt. Phys. **60**, 201 (2011).

[15] See Supplemental Material at http://link.aps.org/supplemental/10.1103/PhysRevLett.114.093002, which includes Refs. [16–18], for details on experimental parameters, the theoretical model, and a calculation of the shot noise limited linewidth.

[16] R. W. P. Drever, J. L. Hall, F. V. Kowalski, J. Hough, G. M. Ford, A. J. Munley, and H. Ward, Appl. Phys. B **31**, 97 (1983).

[17] Z. Ficek and H. S. Freedhoff, Phys. Rev. A **48**, 3092 (1993).

[18] S. Stellmer, R. Grimm, and F. Schreck, Phys. Rev. A **87**, 013611 (2013).

[19] J. Ye, L.-S. Ma, and J. L. Hall, J. Opt. Soc. Am. B **15**, 6 (1998).

[20] L.-S. Ma, J. Ye, P. Dubé, and J. L. Hall, J. Opt. Soc. Am. B **16**, 2255 (1999).

[21] T. W. Hänsch and B. Couillaud, Opt. Commun. **35**, 441 (1980).

[22] A. Tallet, J. Opt. Soc. Am. B **11**, 1336 (1994).

[23] E. Kyrölä and S. Stenholm, Opt. Commun. **22**, 123 (1977).

[24] M. Bishof, X. Zhang, M. J. Martin, and J. Ye, Phys. Rev. Lett. **111**, 093604 (2013).

[25] Y. Y. Jiang, A. D. Ludlow, N. D. Lemke, R. W. Fox, J. A. Sherman, L.-S. Ma, and C. W. Oates, Nat. Photonics **5**, 158 (2011).

[26] J. Millo, D. V. Magalhães, C. Mandache, Y. Le Coq, E. M. L. English, P. G. Westergaard, J. Lodewyck, S. Bize, P. Lemonde, and G. Santarelli, Phys. Rev. A **79**, 053829 (2009).

[27] J. G. Bohnet, Z. Chen, J. M. Weiner, D. Meiser, M. J. Holland, and J. K. Thompson, Nature (London) **484**, 78 (2012).

[28] T. Maier, S. Kraemer, L. Ostermann, and H. Ritsch, Opt. Express **22**, 13269 (2014).